Purdue University

Purdue e-Pubs

Weldon School of Biomedical Engineering Faculty Working Papers

Weldon School of Biomedical Engineering

7-2-2023

Cardiac output and stroke volume from the pneumocardiogram: a new mechanistic insight and practical calculation

Charles F. Babbs

Follow this and additional works at: https://docs.lib.purdue.edu/bmewp

This document has been made available through Purdue e-Pubs, a service of the Purdue University Libraries. Please contact epubs@purdue.edu for additional information.

Cardiac output and stroke volume from the pneumocardiogram: a new mechanistic insight and practical calculation

Charles F. Babbs, MD, PhD

Weldon School of Biomedical Engineering, Purdue University

June 30, 2023

Abstract

This paper presents a new and more complete mechanism for the genesis of the pneumocardiogram—a record of the small oscillations in airflow in the trachea and upper airways accompanying each heartbeat. This signal may be the basis of a simple, inexpensive and noninvasive measure of cardiac stroke volume; however, research into its practical use has languished because of poor understanding of its underlying cause and meaning. This paper explains the genesis of the pneumocardiogram, based upon net changes in intrathoracic blood volume during the cardiac cycle, together with low pass filtering of the volume signal by airway resistance and lung-chest compliance. A novel analytical model of the physics of both blood flow and airflow answers the core question of how the pneumocardiogram is produced, and in turn, how to extract the cardiac output and stroke volume from the pneumocardiographic signal. The approach is tested in a numerical model of the systemic circulation, pulmonary circulation, chest cavity, and lungs. Results show good agreement between predicted and true stroke volume over a wide range of normal and abnormal test conditions, with an average ratio of estimated to true stroke volume of 1.00 in the standard normal model, 0.99 with three times normal airway resistance, 0.82 with one third normal airway resistance, and 0.99 with reduced ventricular contraction time. It is time for the biomedical research community to reconsider practical exploitation of this freely available signal, both in anesthetized or intubated patients, and perhaps even in awake, conscious people using well-sealed face masks.

Key words: anesthesia monitor, airflow, airway resistance, Bourland, cardiac function, cardiac depression, ejection fraction, formula, Geddes, mechanism, monitor, oscillations, pulse, pumping, respiration, unidirectional valves, ventricles, waveform, Wessale.

Introduction

The pneumocardiogram (PNCG) is a graphic record of the oscillations in airflow that occur in the trachea and upper airways associated with each heartbeat. During each diastole or filling of the heart with blood, there is a small positive outward flow of air in the trachea. During each systole or ejection of blood from the heart, there is a larger negative inward flow of air in the trachea. Both systolic and diastolic airflows of the pneumocardiogram are about 2 to 10 percent of the much larger respiratory tidal volume. After placement of an endotracheal tube under anesthesia, both the larger respiratory airflow and the smaller cardiogenic airflow of the pneumocardiogram can be measured, without disrupting breathing, using suitable technology[1]. During normal quiet breathing the pneumocardiogram is clearly evident between breaths.

The pneumocardiogram has been described in the scientific literature since the mid-1800's[2] and was studied intensively in large animals by my late mentor, Leslie A. Geddes and my late colleague, Joe Dan Bourland. The phenomenon was well known to their anesthesiologist colleagues, who often observed fluttering, associated with heartbeats, of the unidirectional airflow valves in anesthesia machines during surgery in intubated patients. Geddes and Bourland, together with then graduate student Jerry Wessale, and with modest help from the present author[2], recorded pneumocardiograms in anesthetized, intubated animals by measuring the pressure difference across a Fleisch #2 air resistor connected to a high sensitivity, wide-bandwidth differential pressure transducer. Figure 1 shows a typical pneumocardiogram from these studies.

In Wessale's animal study the correlation coefficients between the systolic PNCG area and true stroke volume, measured by indicator dilution, ranged from 0.60 to 0.91. However, the magnitude of tracheal airflow averaged only about 0.3 ml of air for every 1 ml of cardiac stroke volume. Retrospectively, there was no correction for low pass filtering in the lungs or for effects of vagal stimulation that could increase airway secretions and airway resistance. At that time we could only speculate as to the reason for the difference between airflow and blood flow, suggesting that there must be "types of factors-either physiological or anatomical, which influence the PNCG-SV relationship"[2]. Today in early 2023, the mechanism generating airflow of the PNCG remains unknown, and a method for determining stroke volume quantitatively from PNCG waveforms remains an open problem.

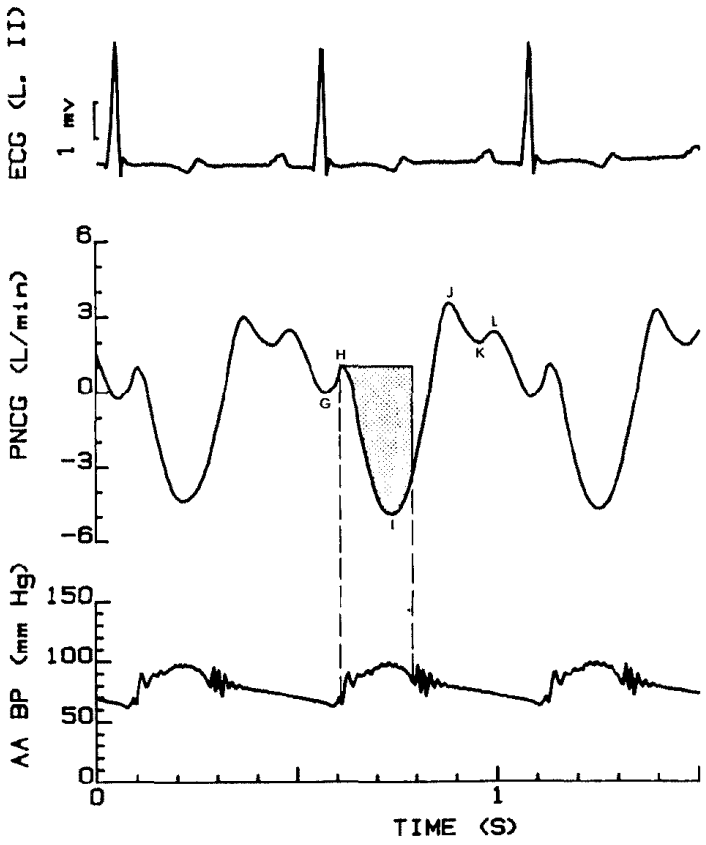

Figure 1: A typical pneumocardiogram from Wessale et al.[2] (middle tracing). The prominent negative wave, indicating inward airflow, is associated with cardiac systole, during the Q-T interval of the companion electrocardiogram (top tracing) and ejection of blood from the heart. The positive phase, indicating outward airflow, is associated with diastolic filling of the heart. The shaded area in the middle tracing was the original index of cardiac stroke volume. Bottom tracing shows blood pressure in the abdominal aorta (AA).

The present paper presents re-formulated and expanded hypothesis, which if confirmed, would explain the genesis, waveform, and magnitude of the PNCG and also allow direct, quantitative estimation of the stoke volume of the heart and the total blood flow, or cardiac output, from the PNCG waveform alone.

Theory

The proposed physical mechanism is that the air flow of the pneumocardiogram is a result of cyclic changes in total blood volume within the thorax produced during each complete heartbeat. This idea for the motor or driver of cardiogenic airflow was anticipated early-on for pressure oscillations measured with the glottis closed[3-5], as well as for the flow based pneumocardiogram with the glottis open[6]. These blood volume changes in turn, slightly squeeze and expand the lungs, and can produce the cardiogenic airflow of the PNCG. What was not fully appreciated earlier is that any resulting air flow signal in the upper airways is blunted or low pass filtered by the total airway resistance and total lung-chest compliance. A related insight is that the resistive and capacitive (RC) properties of the lungs can be easily and practically measured in anesthetized patients, and perhaps extracted directly from the PNCG waveform itself. In particular, the time constant, RC, can be measured as the time constant of exponential decay of airflow after a sigh, and as is routinely done by awake humans every few minutes, and is also done artificially in anesthetized patients to prevent alveolar collapse. With knowledge of both the blood flow mechanism and the RC time constant, together with insights from classical cardiovascular physiology, it appears possible to estimate with good accuracy the total blood flow, or cardiac output, and the stroke volume (cardiac output per heartbeat) on a nearly instantaneous, breath-by-breath basis.

The proposed physical mechanism is demonstrated in Figure 2(a), which shows graphically the balance of inflow and outflow of blood from the chest cavity or thorax. In Figure 2(a) inflow of venous blood during a single heartbeat is represented by the blue colored curve. Outflow of arterial blood is represented by the red colored curve. Because of the high vascular resistance and compliance of the systemic circulation, the rate of blood flow returning to the chest in systemic veins varies less than the rate arterial blood flow exiting the chest to the head and neck via the carotid and vertebral arteries, to the arms via the subclavian and brachial arteries, and to the abdomen and legs via the abdominal aorta.

Importantly, transfer of blood between compartments totally within the thorax, for example from the right ventricle into the pulmonary arteries or from the pulmonary arteries through the pulmonary capillaries and veins into the left atrium, does not change total thoracic blood volume, and hypothetically therefore, would not create a significant influence on the PNCG according to the net blood volume hypothesis. Similarly, coronary artery blood flow, perfusing heart muscle and draining into cardiac veins or Thebesian veins of the heart would not contribute to the PNCG signal. Such cardiac flow amounts to 5 to 7 percent of cardiac output[7]. Similarly, oxygenated arterial flow in the small bronchial arteries to the lungs would not change net thoracic blood volume.

Figure 2(b) illustrates the resulting net change in total thoracic blood volume for one cardiac cycle at steady-state. The net flow is moderately positive during diastole. During ventricular ejection, the sharp negative net flow represents instantaneous outflow of blood from the chest cavity, to the head, neck, arms, abdomen, and legs. Chest wall blood flow to ribs and intercostal muscles does not compress the lungs and is here considered as extra-thoracic.

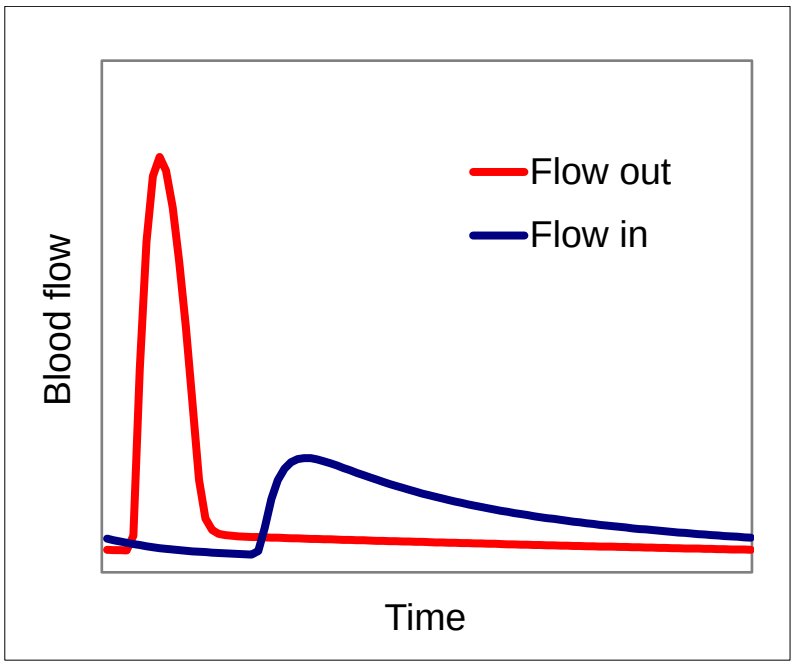

(a)

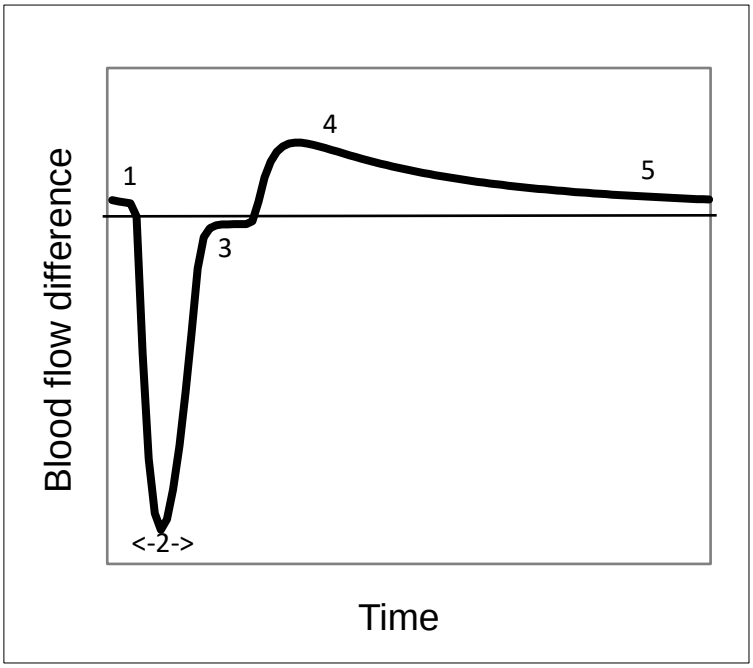

(b)

Figure 2: (a) Balance of inflow and outflow from the thorax. Time zero represents the onset of left ventricular contraction. (b) Difference of inflow minus outflow. Numbers represent classical phases of the cardiac cycle[7]: 1 isovolumic contraction, 2 ventricular ejection, 3 isovolumic relaxation, 4 rapid ventricular filling, 5 slow ventricular filling.

However, it is also important to consider low-pass RC filtering of the blood volume signal in Figure 2(b) by the airway resistance and lung-chest compliance[7]. The time constant of the filter, RC, will be stable over many cardiac cycles. If one can properly understand the effects of RC filtering by the airways and lungs of the net blood volume signal, a practical formula for extraction of stroke volume from a recorded pneumocardiogram may be within reach.

Analytical model

Mechanically the lungs can be regarded as gas filled balloons open to room air via the tracheobronchial tree. For these compartments the cardiogenic change in lung pressure compared to atmospheric pressure is $\Delta P = \Delta V_b/C$, where ΔV_b is the small net blood volume added to the chest, which squeezes an equal volume of air, ΔV_b , into the much larger lung volume, and where C is the combined lung-chest wall compliance. The operative analogy here is pinching or indenting a toy balloon. The small indentation pushes a small volume of air into a much larger volume, slightly increasing the pressure. Releasing the indentation would produce a corresponding decrease in volume and in pressure. Small movements of the handles of a bellows offer another analogy.

With the airway open to zero atmospheric pressure through airway resistance, R, to gas flow, the rate of change in lung pressure may be given by the expression

$$\frac{d\Delta P}{dt} = \frac{1}{C}\left[\frac{\Delta V_b}{dt} - \frac{\Delta P}{R}\right], \tag{1a}$$

or

$$\frac{d\Delta P}{dt} + \frac{\Delta P}{RC} = \frac{1}{C}\frac{\Delta V_b}{dt}. \tag{1b}$$

As an analytical model, let us consider the term dV_b/dt as a half sinusoidal function over the period of ventricular ejection from time 0 to time t_e , such that for constant, a ,

$$\frac{dV_b}{dt} = -a \cdot \sin\left(\frac{\pi}{t_e}t\right). \tag{2}$$

The negative sine in Equation (2) indicates that during ventricular ejection more blood leaves the chest cavity via arteries than returns to the chest cavity via veins. When t = 0 outflow is zero; when $t = t_e$, outflow is also zero; and between these times thoracic outflow is described by a negative half sinusoidal function.

Box 1:

For angular frequency, $\omega = \frac{\pi}{t_e}$, and ejection time t_e, and the ratio of extra-thoracic / total arterial compliance, $\lambda \sim 0.5$, the volume ejected from the thorax is

$$a\int_0^{t_e} \sin\left(\frac{\pi}{t_e}t\right) dt = -\frac{at_e}{\pi}(\cos(\pi) - \cos(0)) = \frac{2a}{\pi}t_e = \int_0^{t_e}(-\Delta V_b)dt = \lambda \cdot SV\ .$$

Hence the absolute value of constant $a = \frac{\lambda\pi}{2t_e}$, and the signed constant $-a = -\frac{\lambda\pi}{2t_e}$.

As shown in Box 1, signed constant, –a , is related to left ventricular stroke volume, SV, and the fraction, λ , of extra-thoracic to total arterial compliance as

$$a = \frac{\lambda\pi}{2t_e}\ SV. \tag{3}$$

The fraction, λ , equals approximately 1.00 minus the fraction of ejected stroke volume that rapidly expands the thoracic aorta, and so remains within the chest cavity. Then substituting Equations (2) and (3) into Equation (1),

$$\frac{d\Delta P}{dt} + \frac{\Delta P}{RC} = -\frac{1}{C}\cdot\frac{\lambda\pi}{2t_e} SV \sin\left(\frac{\pi}{t_e}t\right), \tag{4}$$

or

$$C\frac{d\Delta P}{dt} + \frac{\Delta P}{R} = -\frac{\lambda\pi}{2t_e} SV \sin\left(\frac{\pi}{t_e}t\right). \tag{5}$$

Further, integrating Equation (1b) over the period of ventricular ejection from time 0 to time t_e ,

$$\Delta P(t_e) - \Delta P(0) + \frac{1}{C}\int_0^{t_e}\frac{\Delta P}{R}dt = \frac{1}{C}\int_0^{t_e}\frac{\Delta V_b}{dt}dt = -\frac{\lambda}{C}SV\ , \tag{6}$$

or

$$C\big(\Delta P(t_e) - \Delta P(0)\big) + \int_0^{t_e}\frac{\Delta P}{R}dt = -\lambda \cdot SV\ \ . \tag{7}$$

The term, $\int_0^{t_e}\frac{\Delta P}{R}dt$ is the PNCG area during ejection, which is negative in sign (Figure 1). The PNCG area can be related directly to stroke volume, once the solution to differential equation (4) for $\Delta P(t)$, and in particular for $\Delta P(t_e) - \Delta P(0) < 0$, is specified.

Based on the solution of differential Equation (4) for ΔP(t), as shown in the Appendix,

$$C\big(\Delta P(t_e) - \Delta P(0)\big) = -\lambda \frac{1+e^{-\frac{t_e}{RC}}}{2} \cdot \frac{\pi^2 R^2 C^2}{t_e^2+\pi^2 R^2 C^2} SV\,, \tag{7}$$

and substituting (7) in (6),

$$-\lambda \frac{1+e^{-\frac{t_e}{RC}}}{2} \cdot \frac{\pi^2 R^2 C^2}{t_e^2+\pi^2 R^2 C^2} SV + \int_0^{t_e} \frac{\Delta P}{R}\,dt = -\lambda \cdot SV\,, \tag{8}$$

or

$$-\lambda \cdot SV\left(1 - \frac{1+e^{-\frac{t_e}{RC}}}{2} \cdot \frac{\pi^2 R^2 C^2}{t_e^2+\pi^2 R^2 C^2}\right) = \int_0^{t_e} \frac{\Delta P}{R}\,dt\,, \tag{9}$$

or

$$SV = \frac{-\int_0^{t_e} \frac{\Delta P}{R}\,dt}{\lambda\left(1-\frac{1+e^{-\frac{t_e}{RC}}}{2}\frac{\pi^2 R^2 C^2}{t_e^2+\pi^2 R^2 C^2}\right)}\,. \tag{10}$$

In this expression e = 2.718 is the base of the natural logarithms, time zero represents the onset of ventricular ejection, and time t_e represents the end of ejection. Note that, as expected, when RC = 0 , $SV = -\frac{1}{\lambda}\int_0^{t_e} \frac{\Delta P}{R}\,dt$, and when RC >> t_e , $SV = \frac{0}{0}$, and is undefined. There are no free parameters or arbitrary constants. The terms R and C always appear together, and the product RC represents the time constant for unforced expiration in normal quiet breathing. This value can be estimated either from the exponential decline in airflow after a sigh, from the decline in airflow during slow breathing, or perhaps from the PNCG waveform itself. The arterial compliance ratio, λ , is relatively insensitive to atherosclerosis which similarly affects arteries inside and outside the thorax.

Numerical model

To explore the feasibility of the concepts embodied in Equation (10) a 14-compartment numerical model of the systemic and pulmonary circulations, illustrated in Figure 3, was adapted from previous work[8]. The model of the cardiovascular system shown in Figure 3 was used to simulate the net change in intra-thoracic blood volume during a cardiac cycle, denoted ΔV_b , and in turn, the resulting tracheal airflow. In the model of the circulatory system, relationships among the volumes and pressures in the various vascular compartments are determined by the definition of compliance and by Ohm's Law. The definition of compliance is $C = \Delta V / \Delta P$, where C is compliance of a blood vessel or cardiac chamber, and ΔP is the incremental change in pressure across its wall when ΔV is introduced. Ohm's Law, which relates flow to pressure

and resistance, is $i = (P_1 - P_2)/R$, where $P_1 - P_2$ is the instantaneous difference in pressure across resistance R as flow i occurs. For short, the subscripted variable names, C , in Figure 3 refer to vascular compliances in the circulatory system, not lung-chest compliance as in Equations (1) through (10).

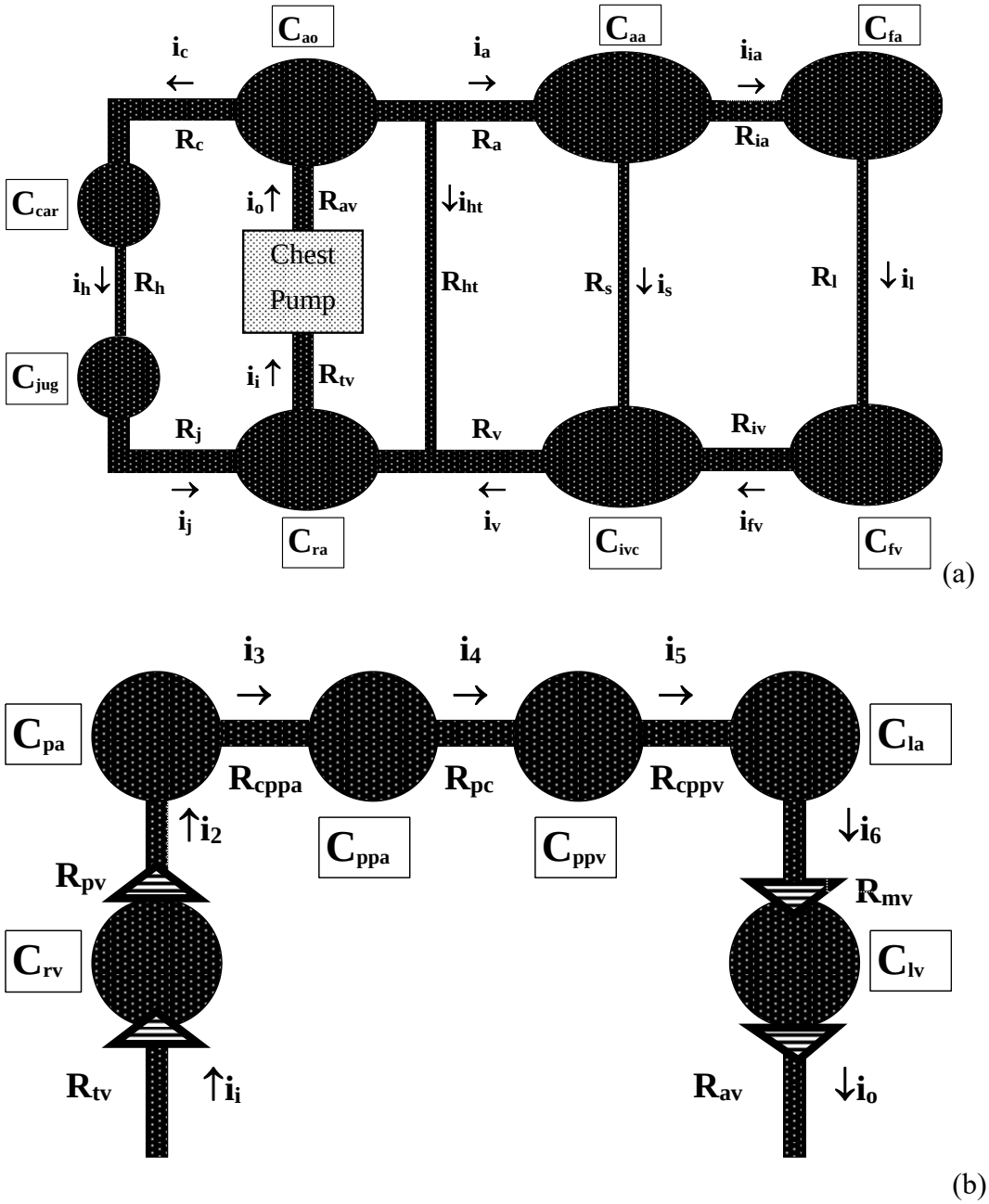

Figure 3: (a) Model of the human circulatory system. (b) Detailed components within the chest. Triangles indicate heart valves. Compliances are denoted C; resistances are denoted R; currents of blood flow are denoted i . Definitions of subscripts indicating anatomic compartments are provided in Table 1. Numerical values of R, and C for the standard normal human circulation are provided in reference [8].

Table 1. Nomenclature for model of the circulatory system

Subscript	Definition
aa	Abdominal aorta
a	Aorta at level of diaphragm
ao	Thoracic aorta
av	Aortic valve
C, car	Carotid
cppa	Central to peripheral pulmonary arteries
cppv	Central to peripheral pulmonary veins
fa	Femoral artery
fv	Femoral vein
h	Head
ht	Heart
ia	Iliac artery
iv	Iliac vein
ivc	Inferior vena cava
j, jug	Jugular
L	Lungs
l	Legs
la	Left atrium and central pulmonary veins
lv	Left ventricle
mv	Mitral valve
pa	Pulmonary arteries (central)
pc	Pulmonary capillaries
ppa	Peripheral pulmonary arteries
ppv	Peripheral pulmonary veins
pv	Pulmonic valve
ra	Right atrium and superior vena cava
s	Systemic circulation below diaphragm
tv	Tricuspid valve
v	Portal and systemic veins at level of diaphragm

Applying these basic concepts with reference to Figure 3 provides a set of governing finite difference equations that can be used to describe hemodynamics. To activate the model, left and right ventricular pressures are augmented by appropriate half-sinusoidal external pressures to mimic cardiac muscle contraction. (Note that the period of the half sine wave representing ventricular muscle contraction is longer than the period of the half sine wave representing ventricular ejection in Equations (2), (4), and (5). The increased duration represents the added time for isovolumic contraction of the ventricles, prior to aortic valve opening, and isovolumic relaxation of the ventricles, after aortic valve closing.)

The differential equations of the form $\Delta P = (i_{in} - i_{out})\Delta t/C$, describing pressure changes in each vascular compartment are integrated numerically to obtain instantaneous pressure vs. time waveforms. Then instantaneous flows, i , between compartments are calculated using Ohm's Law. The coupled respiratory and circulatory models were solved on an ordinary laptop computer to compute time-varying blood pressure and volume changes after a 20 sec stabilization period. Numerical integration was done using the simple Euler method, implemented in Visual Basic code on an ordinary laptop computer, operating under Windows 10. The time step for numerical integration was dt = 0.0001 sec. Full details of the models are provided in reference[8]. The clock time for each individual simulation was less than 2 seconds. A compete code listing is freely available from the author upon request.

Outputs from the model include pressures and volumes in all component vascular compartments, including the cardiac ventricles, major systemic arteries and veins, pulmonary arteries, capillaries, and veins, as well as pressures in the lungs and resulting tracheal airflow. For simplicity, heartbeats occurring between breaths are simulated, eliminating the need for high pass filtering of the signal as would be done in real experimental or clinical settings.

The coupled respiratory and circulatory models allowed the direct, quantitative comparison under a variety of physiologic conditions of estimated stroke volume using Equation (10), with true stroke volume, calculated from the sum of total systemic flows. Test conditions included widely varying ventricular pressures, heart rates, and airway resistances. Such extreme ranges of test conditions, including dangerously low and high stroke volumes, would be difficult to achieve in animal models and unethical to create in humans. The numerical approach, however, provides a safe and convenient way to explore proof of concept.

Signal processing

To determine PNCG curve areas during ejection, the discretized PNCG signal in units of liters/sec was multiplied by each time step, dt = 0.0001 sec, and summed. The starting and stopping criterion were as follows. Integration was started when the PNCG became < 0 and continued until the slope change of the PNCG vs. time curve became positive. This stopping point in the time domain corresponds to the end of the downward spike of the PNCG (point "I" in Figure 1). Preliminary tests showed that this extremum corresponded closely to the end of left ventricular ejection under the widely varying conditions. The negative of the resulting partial PNCG curve area, $-\int_0^{t_e} \frac{\Delta P}{R} \mathrm{dt}$, and the elapsed approximate ejection time, t_e , together with the model time constant, RC, were then used to evaluate Equation (10). Arterial compliance ratio, λ, was calculated for standard adult human values in reference[8].

Results

Figure 4(a) presents the time domain waveforms of cardiovascular pressures in the computational model in mmHg and also the computed pneumocardiogram in units of L/min. The waveform of the simulated PNCG based on net thoracic blood volume changes, is similar to experimentally measured PNCG waveforms such as that shown in Figure 1. Figure 4(b) shows corresponding calculated changes in thoracic blood inflow and outflow for the standard normal model.

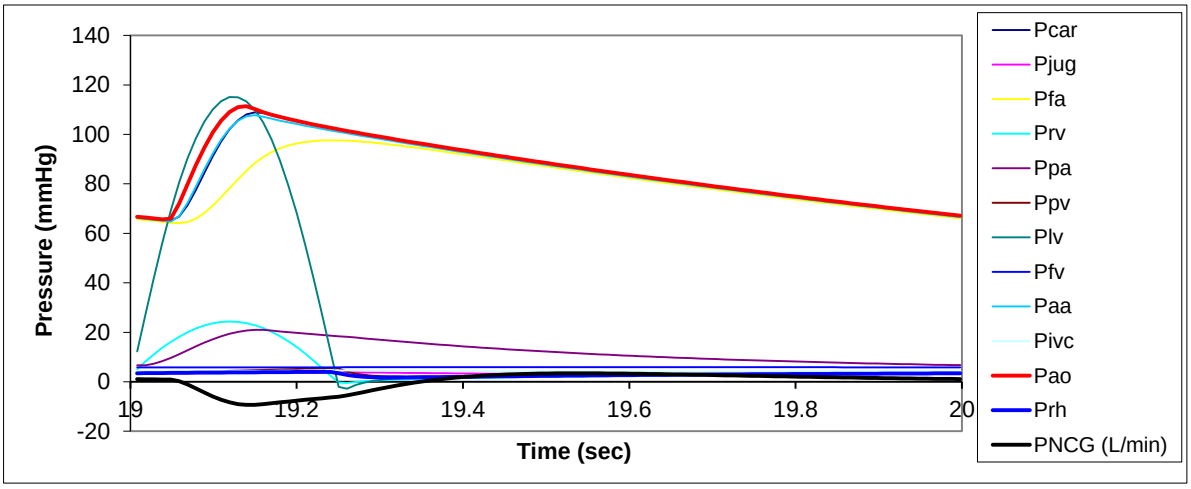

(a)

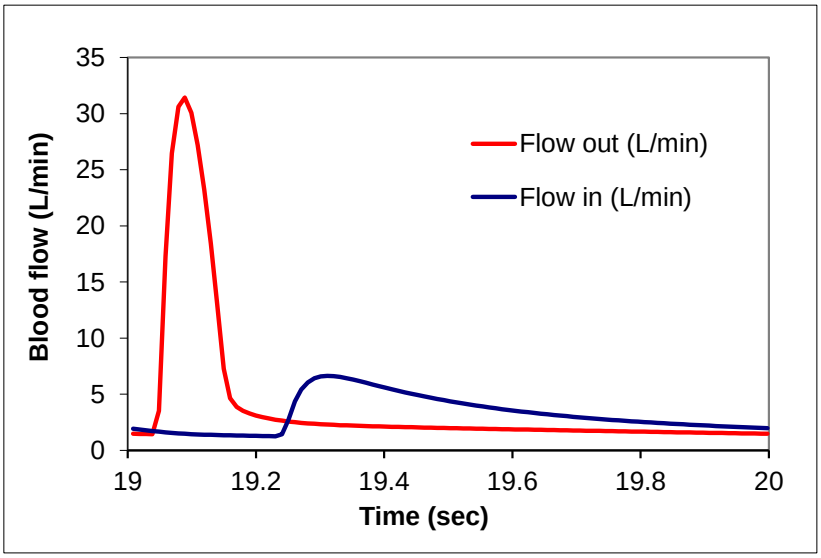

(b)

Figure 4: (a) Simulated cardiovascular pressures (colored curves) and tracheal airflow (solid black curve). On the vertical axis the PNCG is plotted in liters of airflow/min. The horizontal axis is in seconds after the onset of the simulation and complete stabilization of the waveform to a steady-state condition. (b) Simulated changes in thoracic blood inflow and outflow over one steady-state cardiac cycle.

To test the net blood volume hypothesis quantitatively, estimated stroke volume from the PNCG, using Equation (10) was compared with the true stroke volume of blood in the cardiovascular model. Steady-state cardiac output was computed from the sum of resistive flows in all systemic tissue compartments of the model, including the cranial, coronary, and lower body compartments. True stroke volume was computed as steady-state cardiac output divided by cardiac cycle time. A range of stroke volumes was produced in the standard model by varying heart rate from 50 to 250 beats/min. Then with the heart rate at 1 Hz (60/min), a companion series of stroke volumes was simulated by changing peak left ventricular pressure from 40 to 200 mmHg, as peak right ventricular pressure changed proportionally, 25/120 ≈ 0.21 times peak left ventricular pressure.

Figure 5 shows the results for such stroke volume manipulation in the otherwise standard normal model. Estimated stroke volume using Equation (10) is plotted as a function of true stroke volume. Each data point represents a single simulation. The collective data show good agreement of simulated and true values. The 45-degree line represents the line of identity.

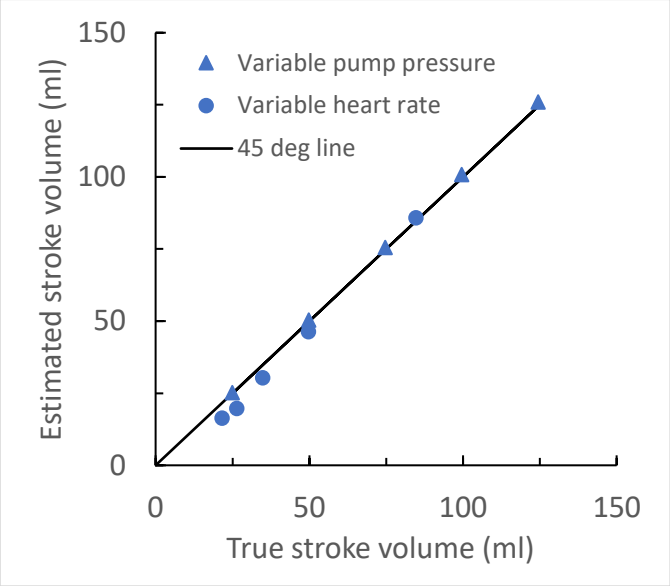

Figure 5. Comparison of estimated cardiac stroke volume from analysis of the pneumocardiogram signal with true stroke volume from analysis of blood flow in a hybrid digital model of the cardiovascular and respiratory systems. Stroke volume was manipulated by changing peak left ventricular pump pressure in steps of 40 mmHg from 40 to 200 mmHg with proportional changes in peak right ventricular pressure (triangles), and also by changing heart rate in steps of 50 beats/min from 50 to 250 beats/min in an otherwise standard normal model.

Figure 6(a) shows similar data under conditions of three times normal airway resistance and, in turn, three times normal RC time constant. Figure 6(b) shows similar data under conditions of one third normal airway resistance and, in turn, one third normal RC time constant. There is reasonable agreement with true stroke volume in the presence of varying airway resistance. With very low airway resistance (Figure 6(b)) the 20 percent underestimation of stroke volume was associated with a 20 percent underestimation of ejection time, based on the PNCG waveform, and therefore incomplete integration of PNCG area over the full ejection period.

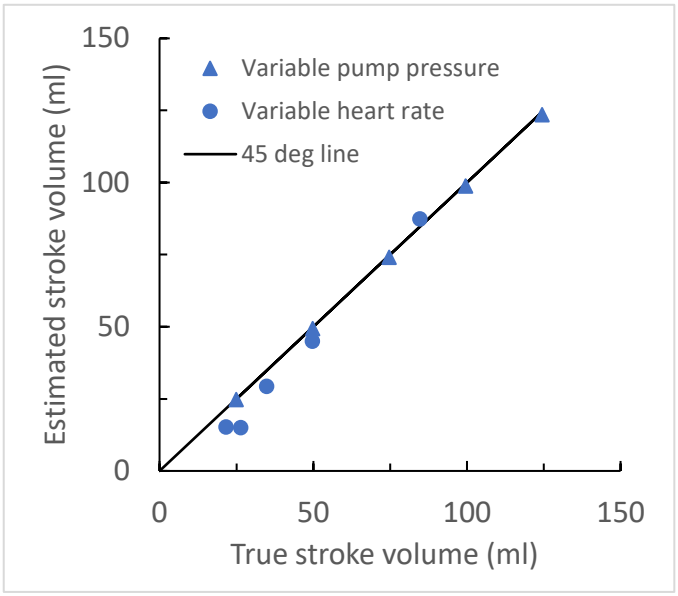

(a)

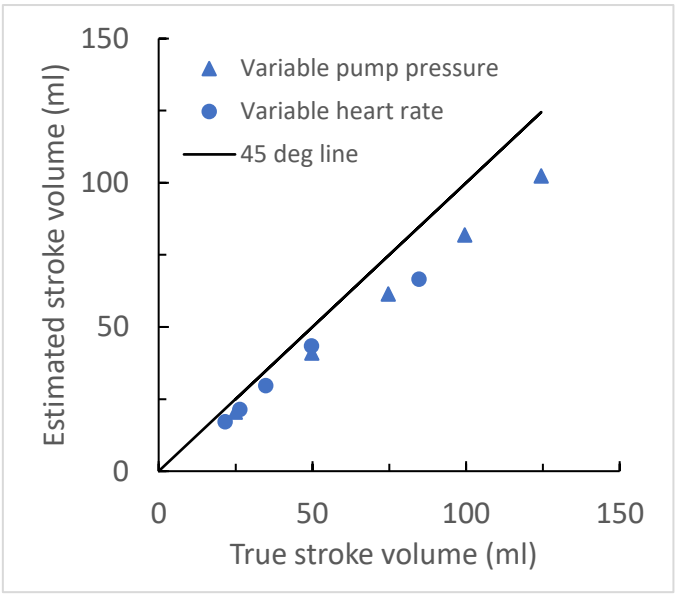

(b)

Figure 6. Calibration functions with (a) high 3X normal airway resistance and (b) one third normal airway resistance. Other details similar to Figure 5.

Figure 7 illustrates the calibration function for an otherwise standard model in which the total duration of ventricular contraction was shortened from one half to one third the total cardiac cycle time. PNCG based estimation of true stroke volume with shorter, more vigorous, ventricular contractions remains accurate.

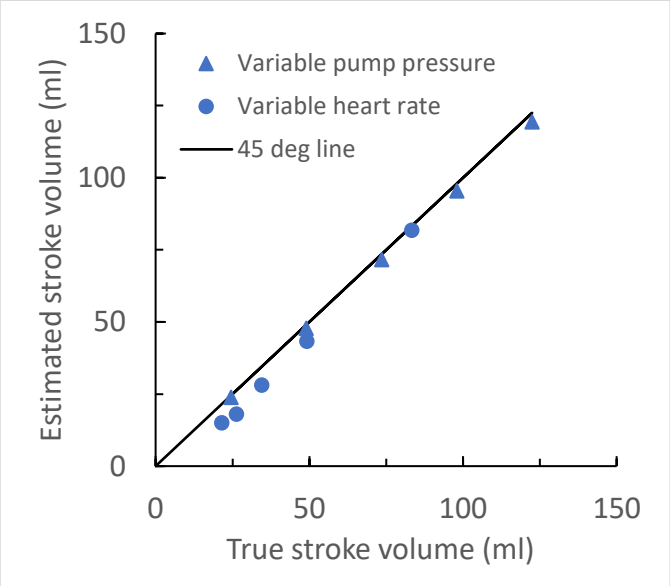

Figure 7. Calibration curves for shortened duration of ventricular squeezing to 2/3 of the standard normal value. Other details similar to Figure 5.

Discussion

The present simulations show that the net blood volume hypothesis explains the pneumocardiogram both qualitatively and quantitatively under a wide variety of physiologic conditions. The simulated PNCG waveform, based on changes in net thoracic blood volume, matches experimental PNCG waveforms in size, shape, and timing, provided that the RC filtering properties of the lungs are taken into account. Cardiac stroke volume calculated from the net positive or outward airflow during ventricular ejection appears accurate for normal, low or high stroke volumes.

Such initial hypothesis testing in silico is reasonable and inexpensive, compared to studies in animals. Experimental manipulations of stroke volume in whole animals include right atrial pacing, vagal stimulation, blood volume augmentation using blood or lactated Ringer's solution, blood volume reduction by controlled hemorrhage, and infusion of isoproterenol alone or in combination with atrial pacing or vagal stimulation[2]. However, such interventions needed to produce high and low stroke volumes for concept testing also introduce confounding variables,

such as adrenergic and vagal reflexes, high levels of stress hormones, and tissue hypoxia, which do not occur in computational models.

The driving mechanism based upon the net change in intrathoracic blood volume is readily deduced from standard human physiology and anatomy[7]. Earlier papers by Blair[5] and Luisada[3] in the 1930's and 40's described the same idea to explain chest pressure oscillations with the glottis closed. Others have used the term pressure pneumocardiogram to refer to these time domain waves[4,9]. The more modern pneumocardiogram, defined in terms of air outflow, can in principle be related directly to the pressure pneumocardiogram. With the glottis closed, decreased net thoracic blood volume during systole decreases lung pressure; while with the glottis open, decreased net thoracic blood volume during systole induces a negative signed inflow of air in the trachea, and vis versa. The waveforms are similar in both the pressure and flow domains[2,3]. However, the flow signal is substantially low pass filtered according to the RC time constant of the airways.

In a follow-up to our original study, Jerry Wessale at Purdue[6] directly studied the relationship between tracheal air flow and induced changes in intrathoracic volume as a basis for calibration of the pneumocardiogram. He used an esophageal balloon, rapidly inflated with volumes of 4 to 36 ml of air to create known positive changes in intrathoracic volume in 19 anesthetized, intubated dogs. The resulting tracheal outflow of air averaged 53% of the known inflow volume, with a correlation coefficient of 0.71. However, as before in our early work, the low pass RC filtering of the signal by the airways was not considered. The present work includes an analytical accounting of the low-pass RC filtering of the primary volume signal by airway resistance and lung compliance. The simulations over a wide range of physiologic and pathophysiologic conditions, which would be hard to create validly in animals, confirm that truly quantitative assessment of stroke volume is possible.

Earlier investigators envisioned that the PNCG might serve as a useful monitor of cardiovascular status during anesthesia[2,6]. Its virtue would be providing information about actual cardiac pumping, in contrast to the electrocardiogram (ECG), which gives information only about electrical triggering of the heart, regardless of pump function. In the 20th Century there was no accounting for RC filtering of the signal, leading to the conclusion that, at best, the PNCG could track changes in stroke volume, but not measure stroke volume quantitatively. Since then, Nazmi Yılmaz and coworkers[10] have used more advanced mathematics, including nonlinear analysis, to extract meaningful information from the pneumocardiogram. They recorded (inverted) pneumocardiogram signals using a miniature Fleisch transducer in nine pentobarbital anesthetized rats and processed the signals using Boltzmann Gibbs entropy, maximum Lyapunov exponents, and a scale index method based on wavelet transforms. In contrast, the present approach to analysis of the PNCG focuses upon a better understanding of the underlying physiology, anatomy, and biophysics, together with simpler, calculus-based mathematics.

Further engineering research and development are needed to identify the best practical approach to acquisition of this freely available signal in a cost-effective way that is compatible with normal clinical routines. Modern technology may make measurement of the pneumocardiogram simpler and easier than in the past. The downstream applications of a simpler, lower cost PNCG are significant. In addition to monitoring closed-chest anesthetized patients, one can imagine

acquiring a useable pneumocardiogram in awake, conscious patients with soft, well-sealed face mask, after the patient is instructed to breathe in and out slowly through an open mouth with throat relaxed (to help maintain an open glottis). In that case the PNCG could become a routine office procedure, similar to pulse oximetry. Mechanical prototyping and testing will be needed to find the best and most cost-effective airflow transducers for particular applications.

In addition to allowing monitoring of anesthetized patients without endotracheal tubes, face mask pneumocardiography after treadmill exercise could supplement noninvasive cardiovascular evaluations for possible heart disease. Perfect absolute calibration might not be needed. The percent increase in PNCG based cardiac output with standardized exercise could serve as a simple metric of heart health vs. disease. A similar system might also be used in sports medicine and athletic training as a measure of cardiovascular fitness in elite athletes. The practical feasibility of such short duration testing in awake patients has already been demonstrated by Lauzon 1998 and coworkers[11], who measured cardiogenic oscillation phase relationships during single-breath tests.

The present concept testing with mathematical models is obviously preliminary and subject to refinement and practical experimental confirmation. Further work in PNCG signal processing is needed to identify the best way to estimate time constant, RC, for a particular subject. Options include measuring the time required for exponential decline in airflow to 37% (1/e) of the initial value either during an induced sigh, during a normal exhalation, or perhaps even during the terminal phase of the PNCG waveform itself. As shown by the results in Figure 6(b), a better way is needed to extract ejection time from the PNCG waveform in cases of abnormally low airway resistance. Additionally, some type of routine high pass filtering will likely be needed to separate the purely cardiac signals from the larger respiratory flows.

Nevertheless, with low-cost, compact digital signal processing now available and with improved understanding of the genesis of the pneumocardiogram, it is time to reassess the value of the PNCG as an easily acquired, painless, non-invasive measure of minute-by-minute cardiac output and stroke volume. Including the quantitative effects of RC filtering, as shown here, may seem a modest improvement, but it is a big step in improving accuracy of stroke volume estimates from the pneumocardiogram.

Appendix: solution of the governing differential equation

To solve

$$\frac{d\Delta P}{dt} + \frac{\Delta P}{RC} = -\frac{\lambda}{C} \cdot \frac{\pi}{2t_e} \sin\left(\frac{\pi}{t_e} t\right), \tag{11}$$

or lumping constants,

$$\frac{d\Delta P}{dt} + \frac{\Delta P}{RC} = -k \cdot \sin\left(\frac{\pi}{t_e} t\right), \tag{12}$$

use Grossman's exact solution[12] to the ordinary differential equation $\frac{d\Delta P}{dt} + a(t)\Delta P = b(t)$, for which

$$\Delta P(t) = e^{-\int_0^t a(t)dt} \cdot \int_0^t \left(e^{+\int_0^t a(t)dt} \cdot b(t) \right) dt + C^* e^{-\int_0^t a(t)dt}, \tag{13}$$

as is easily confirmed by differentiation of Equation (13). Then for the initial condition that constant of integration, C* = ΔP(0) at t = 0

$$\Delta P(t_e) - \Delta P(0) = -e^{-\int_0^{t_e} \frac{1}{RC} dt} \cdot \int_0^{t_e} \left(e^{+\int_0^{t_e} \frac{1}{RC} dt} \cdot k \sin\left(\frac{\pi}{t_e} t\right) \right) dt, \tag{14}$$

$$\Delta P(t_e) - \Delta P(0) = -e^{-\frac{t_e}{RC}} \cdot \int_0^{t_e} \left(e^{+\frac{t}{RC}} \cdot k \sin\left(\frac{\pi}{t_e} t\right) \right) dt. \tag{15}$$

Consulting a table of integrals[13], $\int e^{Ax} \sin(bx)\, dx = \frac{e^{Ax}}{A^2+B^2} [A\sin(Bx) - B\cos(Bx)]$. So

$$\Delta P(t_e) - \Delta P(0) = \frac{k \cdot e^{-\frac{t_e}{RC}}}{\frac{1}{R^2C^2} + \frac{\pi^2}{t_e^2}} \left\{ e^{+\frac{t_e}{RC}} \left(\frac{1}{RC} \sin(\pi) - \frac{\pi}{t_e} \cos(\pi) \right) - e^0 \left(\frac{1}{RC} \sin(0) - \frac{\pi}{t_e} \cos(0) \right) \right\} \tag{16}$$

$$\Delta P(t_e) - \Delta P(0) = \frac{k \cdot e^{-\frac{t_e}{RC}}}{\frac{1}{R^2C^2} + \frac{\pi^2}{t_e^2}} \cdot \left\{ e^{+\frac{t_e}{RC}} \cdot \left(\frac{\pi}{t_e} \right) + \frac{\pi}{t_e} \right\}, \tag{17}$$

$$\Delta P(t_e) - \Delta P(0) = k \frac{\frac{\pi}{t_e} + \frac{\pi}{t_e} e^{-\frac{t_e}{RC}}}{\frac{1}{R^2C^2} + \frac{\pi^2}{t_e^2}}. \tag{18}$$

Now expand the constant $k = \frac{\pi}{2t_e} \frac{\lambda}{C} SV$ and simplify.

$$\Delta P(t_e) - \Delta P(0) = -\frac{\pi}{2t_e} \frac{\lambda}{C} SV \frac{\frac{\pi}{t_e}\left(1 + e^{-\frac{t_e}{RC}}\right)}{\frac{1}{R^2C^2} + \frac{\pi^2}{t_e^2}} = -\frac{1}{2} \frac{\lambda}{C} SV \frac{\frac{\pi^2}{t_e^2}\left(1 + e^{-\frac{t_e}{RC}}\right)}{\frac{1}{R^2C^2} + \frac{\pi^2}{t_e^2}}, \tag{19}$$

$$\Delta P(t_e) - \Delta P(0) = -\frac{1}{2}\frac{\lambda}{C} SV \frac{\pi^2 R^2 C^2 \left(1+e^{-\frac{t_e}{RC}}\right)}{t_e^2 + \pi^2 R^2 C^2}, \quad (20)$$

and

$$C\left(\Delta P(t_e) - \Delta P(0)\right) = -\lambda \frac{1+e^{-\frac{t_e}{RC}}}{2} \cdot \frac{\pi^2 R^2 C^2}{t_e^2 + \pi^2 R^2 C^2} SV\ . \quad (21)$$

References

1. Miller MR, Pincock AC (1986) Linearity and temperature control of the Fleisch pneumotachograph. J Appl Physiol (1985) 60: 710-715.
2. Wessale JL, Bourland JD, Babbs CF, Milewski RC, Rockenhauser ME, et al. (1985) Correlation of the cardiogenic air flow in the respiratory airway (i.e. the pneumocardiogram) with left ventricular stroke volume in dogs. Jpn Heart J 26: 777-785.
3. Luisada A (1942) The Internal Pneumocardiogram. American Heart Journal 23: 676-691.
4. Heckman JL, Stewart GH, Tremblay G, Lynch PR (1982) Relationship between stroke volume and pneumocardiogram. J Appl Physiol Respir Environ Exerc Physiol 52: 1672-1677.
5. Blair HA, Wedd AM (1939) The measurement of in man by a pneumocardiographic method of the excess of arterial outflow from the chest over venous inflow during the heart cycle. American Heart Journal 17: 536-541.
6. Wessale JL, Bourland JD, Geddes LA (1988) Relationship between tracheal air flow and induced changes in intrathoracic volume. A basis for calibration of pneumocardiogram. Jpn Heart J 29: 99-106.
7. Boron WF, Boulpaep EL (2005) Medical Physiology. Philadelphia: Elsevier. 1319 p.
8. Babbs CF (2005) Effects of an impedance threshold valve upon hemodynamics in standard CPR: studies in a refined computational model. Resuscitation 66: 335-345.
9. Bijaoui E, Baconnier PF, Bates JH (2001) Mechanical output impedance of the lung determined from cardiogenic oscillations. J Appl Physiol (1985) 91: 859-865.
10. Yilmaz N, Akilli M, Ozbek M, Zeren T, Akdeniz KG (2020) Application of the nonlinear methods in pneumocardiogram signals. J Biol Phys 46: 209-222.
11. Lauzon AM, Elliott AR, Paiva M, West JB, Prisk GK (1998) Cardiogenic oscillation phase relationships during single-breath tests performed in microgravity. J Appl Physiol (1985) 84: 661-668.
12. Grossman SI (1981) Calculus. New York: Academic Press. 1020 p.
13. Selby SM (1975) CRC Standard Mathematical Tables. Cleveland. 756 p.